Spectroscopic Characterization of Heterogeneous Structure of *Samia cynthia ricini* Silk Fibroin Induced by Stretching and Molecular Dynamics Simulation

Mingying Yang, Juming Yao, Masashi Sonoyama, and Tetsuo Asakura*

Department of Biotechnology, Tokyo University of Agriculture and Technology, Koganei, Tokyo 184-8588, Japan

Received February 1, 2004; Revised Manuscript Received March 8, 2004

ABSTRACT: The ^{13}C CP/MAS NMR, X-ray diffraction, and Raman spectroscopies were used for monitoring the structural transition of *Samia cynthia ricini* (*S. c. ricini*) silk fibroin induced by stretching. Here the silk fibroin was obtained from the aqueous solution stored in the silk gland. All of these spectroscopic data indicate that the structural transition from α-helix to *β*-sheet occurs with increasing the stretching ratio, especially between the stretching ratios, ×4 and ×6. The ^{13}C chemical shifts of Ala C*β* peak in the ^{13}C CP/MAS NMR spectrum change significantly depending on α-helix, random coil, and two kinds of *β*-sheet structure, which make it possible to clarify the local structure and structural transition. Actually, the fraction of individual structure in the silk fibroin samples was determined from decomposition of the Ala C*β* peak by assuming a Gaussian line shape. To examine the conformational change of Ala residues of the polyalanine region in *S. c. ricini* silk fibroin observed with these spectroscopic methods, MD simulations for four peptide molecules, AGGAGG(A)$_{12}$GGAGAG, with α-helix conformation were performed in the presence of water molecules under different tensile strengths, and then additional MM calculations were performed after removal of water molecules. The change in the conformational character of Ala residues induced by stretching is explicable by these calculations.

Introduction

There are many kinds of silks from silkworms and spiders with different structures and properties.[1] *Samia cynthia ricini* (*S. c. ricini*) is a wild silkworm, and the primary structure has recently been determined by Yukuhiro et al.,[2] which was very similar to the primary structure of silk fibroin from other wild silkworm, *Antheraea pernyi* (*A. pernyi*).[3,4] Namely, the silk fibroin mainly consists of the repeated similar sequences by about 100 times where there are alternative appearance of the polyalanine (PLA) region, (Ala)$_{12-13}$ and Gly-rich region.

The structure of *S. c. ricini* silk fibroin in aqueous solution has been studied with solution ^{13}C and ^{15}N NMR.[5−8] The fast exchange in the NMR time scale between helix and coil forms of the PLA region has been observed during the helix-to-coil transition with changing temperature. On the other hand, most of the glycine residues keep a random coil conformation during the helix−coil transition of the PLA region. However, slow exchange between helix and coil forms in the NMR time scale was observed exclusively for the glycine residue (italics) in the Gly-*Gly*-(Ala)$_{12-13}$ sequence.[8] Thus, the solution NMR can be used for studying the structural change between α-helix and random coil forms of the silk fibroin for each residue selectively together with the change in the exchange rate between both forms. The monitoring of the structural change from α-helix (in solution state) to *β*-sheet (in solid state) of the silk fibroin was possible with alternative NMR observations between ^{13}C DD/MAS (solution state) and ^{13}C CP/MAS (solid state).[9]

The solid-state NMR method has been used for study of the solid-state structure of *S. c. ricini* silk fibroin and the model peptides.[10−15] The silk fibroin dried gently after taking out from the silk gland shows a typical α-helix pattern. Recently, our solid-state NMR studies[14,15] point out that Ala residues at the N- and C-terminus of PLA regions take a slightly different helix and contribute to the formation of $i \rightarrow i + 3$ hydrogen bonding. This special conformation seems to stabilize the α-helix formation of the PLA region. On the other hand, the silk fibroin fiber shows *β*-sheet chemical shifts of Ala carbons in the ^{13}C CP/MAS NMR spectrum. The ^{15}N and ^{13}C labelings of Ala and Gly residues of *S. c. ricini* silk fiber were performed for the detailed structural study of these residues.[12] The fraction of the oriented Ala domain in the silk fiber was determined as 75%, while that of the oriented Gly domain was 65%. The torsion angles of the oriented Ala and Gly residues were determined to be $(\varphi, \psi) = (-130 \pm 10°, 140 \pm 10°)$ for both residues, which is typical torsion angles of antiparallel *β*-sheet structure. The DOQSY (double-quantum/single-quantum correlation experiment) method has also been used to determine the torsion angles of Ala residue precisely for [1-^{13}C]Ala-*S. c. ricini* silk fibroin film and fiber. The torsion angles were determined to be $(\varphi, \psi) = (-60°, -45°)$ for the film and $(-135°, 150°)$ for the fiber.[13] Recently, we have determined the structure of silk fibroin fiber of a well-known domestic silkworm, *Bombyx mori* (*B. mori*), using solid-state NMR methods in detail.[16,17] ^{13}C CP/MAS NMR gives detailed information on the heterogeneous structure through the analysis of broad and asymmetric peak observed for the Ala C*β* carbon of *B. mori* silk fibroin fiber and the crystalline fraction.[17] The fractions of various heterogeneous components in *B. mori* silk fibroin fiber were determined from their relative intensities after the peak decomposition.

The molecular dynamics (MD) calculation has been used to simulate the structural change of Poly(Ala-Gly)

* Corresponding author: Tel & FAX: +84-42-383-7733; e-mail asakura@cc.tuat.ac.jp.

10.1021/ma049787u CCC: $27.50
Published on Web 04/09/2004

as a model for the crystalline fraction of *B. mori* silk fibroin, from silk I (repeated β-turn type II) to silk II (heterogeneous structure, but mainly antiparallel β-sheet), and to clarify the detailed mechanism of the silk fiber formation.[18,19] The structural change during the MD simulation occurs easily by taking into account several external forces (the presence of water molecules around the silk chains and application of both shear and tensile stresses to the silk fibroin) applied to the silk fibroin simultaneously. The heterogeneous structure of the silk fiber determined with solid-state NMR could be reproduced well with the MD calculation and then additional molecular mechanics (MM) calculation after removal of water molecules.[19] Thus, MD calculation is a powerful method to study the character of the local structure of the amino acid residues in silk fibroins and to monitor the structural change induced by external forces.

In this paper, we tried to study the structural transition of *S. c. ricini* silk fibroin induced by stretching of the sample prepared from the silk fibroin stored in the silk glands of the silkworms. To monitor the structural change by the stretching, X-ray diffraction, FT-Raman, and ^{13}C solid-state NMR methods were used. The heterogeneous structure of the silk fibroin observed by stretching was studied in detail from the analysis of the Ala Cβ peak in the ^{13}C CP/MAS NMR spectra. Then we applied the MD simulation to study the structural transition of *S. c. ricini* silk fibroin and to reproduce the heterogeneous structure in PLA region by stretching.

Materials and Methods

***S. c. ricini* Silk Fibroin Samples with Different Stretching Ratio.** *S. c. ricini* silkworms were reared in our laboratory. The 7-day-old fifth instar larvae were anesthetized in the ice-cold water for 10 min. The posterior divisions of silk glands were pulled out with forceps from a small incision on the abdominal side of the bead−thorax intersegment. Then, the silk glands were washed repeatedly in ice-cold 1.15% potassium chloride solution. After immersing them in the dilute acetic acid (0.1%) for 10 min, the silk glands were washed carefully by gently agitating the acid solution to remove contaminants such as gland epithelium. Before stretching treatment, the silk glands were washed by 1.15% potassium chloride solution again to remove acetic acid attached on the silk glands. The silk fibroin samples stored in the silk glands were stretched to the required stretching ratio at room temperature by keeping stretching rate 5−10 cm/s.[20] The ends of the stretched silk samples were then fixed on the stretching apparatus to prevent the relaxation and dried at room temperature for 1 day prior to the X-ray, Raman, and NMR observations.

***S. c. ricini* Silk Fibroin Fiber from Cocoon.** The cocoons of *S. c. ricini* were degummed three times with 0.1% (w/w) sodium peroxide (Na_2O_2) solution at 100 °C for 30 min and washed with distilled water in order to remove silk sericin, another silk protein, from the surface of silk fibers. The fibroin fibers were dried at 37 °C overnight prior to the next experiment.

X-ray Diffraction Measurement. The X-ray detector system employed in these measurements was UltraX-18. The voltage and current of the generator were set at 50 kV and 250 mA, respectively. The image project DIP-100s was used for sample−detector distance of 75 mm.

FT-Raman Measurement. Near-infrared (NIR) Fourier transform (FT) Raman spectra were obtained by means of a Bruker FRA-106 Raman module coupled to an IFS-66 FT-spectrophotometer. An Nd:YAG laser (1064 nm) was used as the exciting source.

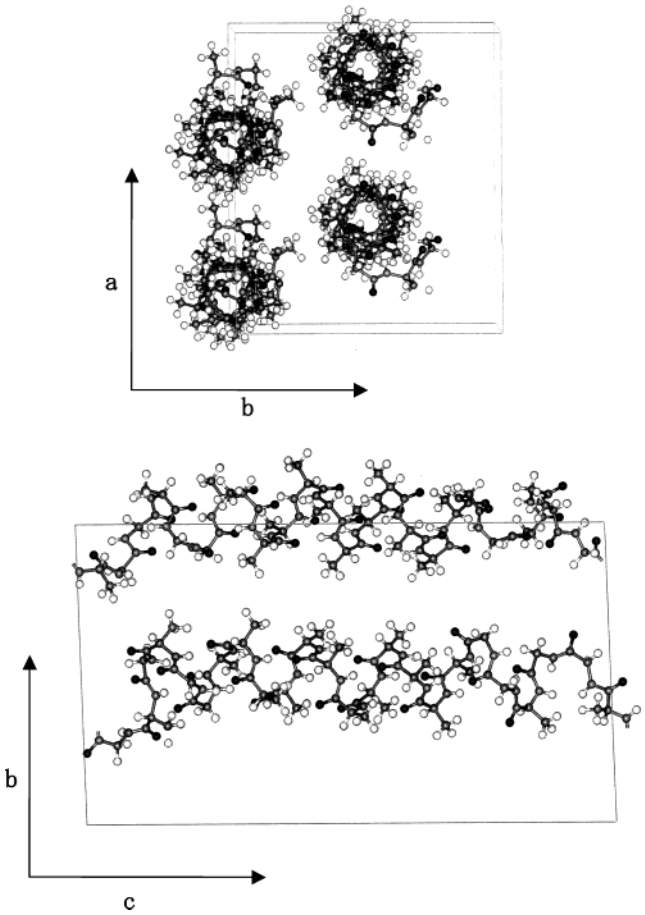

Figure 1. Initial arrangement of the peptide, AGGAGG-$(A)_{12}$GGAGAG, chains before MD simulation (water molecules are included, but not shown here).

^{13}C CP/MAS NMR Measurement. ^{13}C CP/MAS spectra were acquired on a Chemagnetics CMX-400 spectrometer operating at 100 MHz, with a CP contact time of 1.5 ms, TPPM (two-pulse phase-modulated) decoupling, and magic angle spinning at 5 kHz. A total of 50 000−100 000 scans were collected over a spectral width of 80 kHz, with a recycle delay of 0.5 s. Chemical shifts were reported in ppm relative to TMS as a reference.

MD and MM Calculations of the Model Peptide. Several series of MD and MM calculations were performed by using "Discover 3" module in Insight II (4.0.0P+, Accelrys Inc.) on an OCTANE workstation (Silicon Graphics Inc.).[19] All of the calculations and preparation for initial structures were performed by using some of the modules in Insight II. Initially the peptide, AGGAGG$(A)_{12}$GGAGAG, was designed as a model of the PLA region, YGGDGG$(A)_{12}$GGAGDG in *S. c. ricini* silk fibroin.[2] Thus, in this study, Ala residue was used instead of Asp and Tyr residues during MD simulation. Four AGGAGG-$(A)_{12}$GGAGAG chains with α-helix form were used for the initial arrangement of the chains in the aqueous solution system. The periodic cell contained 351 water molecules which correspond to the concentration of silk fibroin in the silk gland (about 30%). The preparation of the system is as follows. Four AGGAGG$(A)_{12}$GGAGAG chains with α-helix form were placed in a periodic boundary cell homogeneously by using "crystal cell" module in Insight II, but the water molecules are not in the equilibrium state. The MD simulations were continued until reaching the equilibrium state (equilibrium stage; 5000 steps) without any external forces. Figure 1 shows the initial structure of these model peptides used for MD in the cell vector (*a*,*b*,*c*), where the water molecules are not shown. The Parrinello and Rahman method[21] was used for the MD simulation under tensile stress, and tensile stress was set at 0.1, 0.3, 0.5, 0.8, and 1.0 GPa, which are parallel to the fiber. The velocity

Velret algorithm was used to integrate Newton's equation of motion (with a time step of 1.0 fs).[22] Temperature of the systems was controlled by the Andersen method at 298 K.[23] The calculations continued under tensile stress (simulation stage; 200 000 steps, that is, 200 ps). The snapshot structures were sampled 20 steps during the latter steps from 80 to 100 ps in the simulation stage. All of the simulations were performed by using pcff force field (Accelry Inc.). Nonbonded interactions were calculated using 9.5 Å cutoff distance. After removal of water molecules, MM calculation was performed under different tensile stress, 0.1, 0.3, 0.5, 0.8, and 1.0 GPa.

The conformational probability distributions of the Ala residues in the model peptide chains were calculated at the equilibrium stage and after MD calculations under external forces.[19] Backbone torsion angles of Ala residue, Ala(ϕ,ψ), were extracted from the trajectory of each simulation and used for the calculation of preparing the histograms of conformations $N(\phi \pm 10°, \psi \pm 10°)$. Here $N(\phi \pm 10°, \psi \pm 10°)$ means the number of conformers with torsion angles: $(\phi \pm 10°, \psi \pm 10°)$. The conformational probability $P(\phi,\psi)$ of Ala residues was calculated according to the following equation:[24]

$$P(\phi,\psi) = \frac{N(\phi \pm 10°, \psi \pm 10°)}{N_{\text{total}}}$$

where N_{total} means the total number of conformations of Ala residue in the trajectory. The conformational probabilities $P(\phi,\psi)$ were plotted against the torsion angles, ϕ and ψ.

Results and Discussion

Structural Transition of *S. c. ricini* Silk Fibroin with Stretching Monitored Using X-ray Diffraction and Raman Methods. The monitoring of the structural change of *S. c. ricini* silk fibroin induced by stretching was first performed with the X-ray diffraction method. The change in the X-ray diffraction patterns is shown in Figure 2. There are no obvious oriented patterns for the samples with the stretching ratio from ×2.5 to ×4, and only the lines of 4.0 and 7.2 Å were observed. These lines indicate that the main conformation of *S. c. ricini* silk fibroin is the α-helix.[25] The orientation is clearly observed for the sample with the stretching ratio ×6 by the observation of the lines, 1.82, 2.22, 3.6, 4.3, and 5.1 Å. This is an oriented pattern with β-sheet structure of the silk.[26] With further increasing the stretching ratio from ×8 to ×10, similar oriented patterns were observed. Thus, the X-ray diffraction analysis indicates that a remarkable structural transition from α-helix to β-sheet occurs between the stretching ratio ×4 and ×6. Such a structural change of *S. c. ricini* silk fibroin induced by stretching has been also observed for *A. pernyi* with the X-ray diffraction method:[27] *A. pernyi* silk fibroin also takes a remarkable structural transition from α-helix to β-sheet at the stretching ratio ×6, and small amounts of α-helix still exist even at the stretching ratio ×12. Recently, we found that *A. pernyi* silk fibroin without stretching takes mainly the α-helix form, with the coexistence of a few random coil forms.[28]

Raman spectroscopy can make an original contribution to the study of silk fibroins and of their conformational transitions. The silk I and silk II forms of *B. mori* silk fibroin have been extensively studied by Raman spectroscopy. Monti et al.[29] compared the Raman spectra between silk I and silk II forms from the Raman markers besides amide I and amide III modes and proposed silk I and random coil forms for the silk film prepared from liquid silk. In this work, we applied the FT-Raman method to monitoring the structural transition of *S. c. ricini* silk fibroin induced by stretching. The

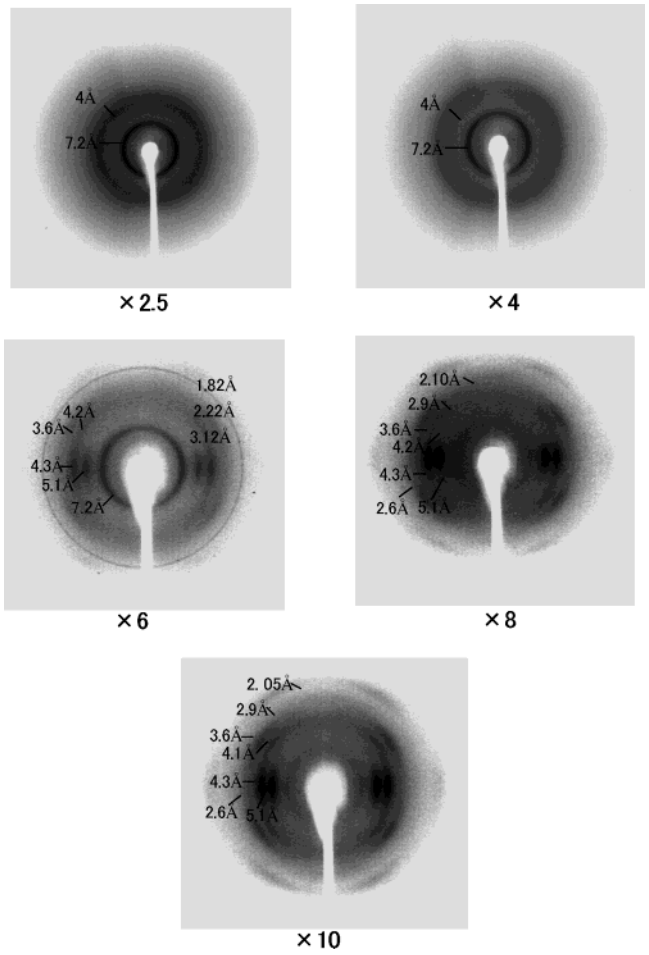

Figure 2. X-ray diffraction patterns of *S. c. ricini* silk fibroin samples with different stretching ratio (×2.5, ×4, ×6, ×8, and ×10).

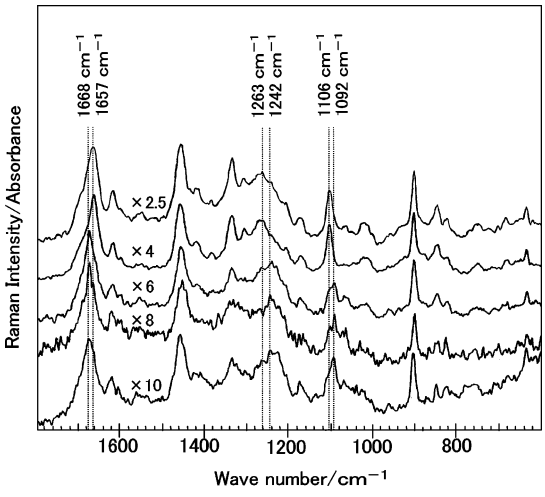

Figure 3. FT-Raman spectra of *S. c. ricini* silk fibroin with different stretching ratio (×2.5, ×4, ×6, ×8, and ×10).

Raman spectra of *S. c. ricini* silk fibroin were observed for the samples with different stretching ratios from ×2.5 to ×10, as shown in Figure 3. The amide I and amide III regions were used for monitoring the structural change. The amide I at 1657 cm^{-1} and amide III at 1263 cm^{-1} are characteristic of α-helical and/or random coil structure.[30] Thus, the observation of the peaks at 1657 cm^{-1} in amide I and 1263 cm^{-1} in amide III of the samples with stretching ratios ×2.5 and ×4

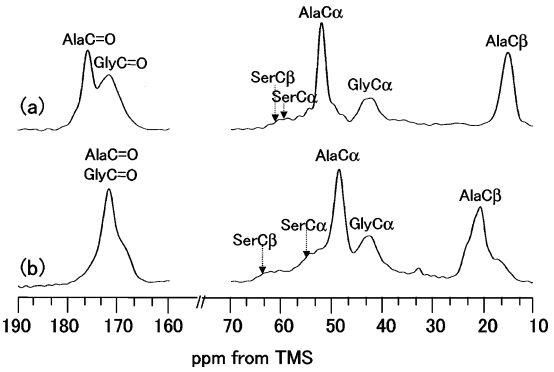

Figure 4. ^{13}C CP/MAS NMR spectra of (a) *S. c. ricini* silk fibroin film without stretching and (b) *S. c. ricini* silk fibroin fiber prepared from the cocoon.

Table 1. ^{13}C CP/MAS NMR Chemical Shifts of *S. c. ricini* Silk Fibroin Film without Stretching and *S. c. ricini* Silk Fibroin Fiber Prepared from Cocoon

	chemical shift (ppm)	
carbon in amino acids	*S. c. ricini* silk fibroin film	*S. c. ricini* silk fibroin fiber
Ala Cα	52.0	48.8
Ala Cβ	15.7	20.8
	17.5	22.8
		15.7
		17.5
Ala C═O	176.4	171.9
Ser Cα	59.2	54.9
Ser Cβ	60.7	63.4
Tyr Cα	55.0	55.0
Gly Cα	42.7	42.8
Gly C═O	171.3	171.9

indicates that structure is mainly α-helix besides random coil. However, the *S. c. ricini* silk fibroin with stretching ratio more than ×6 together with fiber exhibits different Raman spectra from sample with stretching ratios ×4 by judging from position and intensity of the peaks. The amide I peak is shifted from 1657 to 1668 cm^{-1}, and the peak at 1263 cm^{-1} decreases and a new peak at 1242 cm^{-1} increases. In addition, a remarkable intensity change was also observed in the spectral region below 1200 cm^{-1}. A new peak at 1092 cm^{-1} appears with decreasing peak intensity of 1106 cm^{-1}. Such similar Raman spectra were also observed in *A. pernyi* silk fibroin films when the structural transition from α-helix to β-sheet occurs.[31,32] Thus, Figure 3 indicates that the structural transition from α-helix to β-sheet occurs remarkably at the stretching ratio between ×4 and ×6, which is the same tendency as X-ray diffraction observation mentioned above.

Structural Transition of *S. c. ricini* Silk Fibroin with Stretching Monitored Using the ^{13}C CP/MAS NMR Method. ^{13}C CP/MAS NMR spectra of *S. c. ricini* silk fibroin in the both forms without stretching (a) and the silk fiber (b) are shown in Figure 4, and the chemical shifts of *S. c. ricini* silk fibroin film and fiber are summarized in Table 1. The silk fibroin without stretching indicates that the Ala residues in the PLA chain take exclusively the α-helix structure. This is derived from the chemical shift, 15.7 ppm, of the Ala methyl peak as reported previously.[11−15] On the other hand, by judging from the chemical shift values of three Ala carbons (Cα, Cβ, and carbonyl carbon), the Ala residues in the silk fiber take mainly β-sheet structure. In addition, the Ser Cα and Cβ peaks shifted from 59.2, 60.7 ppm (α-helix) to 54.9, 63.4 ppm (β-sheet), respectively, although the peaks were broad.[28] Thus, the structural transition from α-helix to β-sheet occurs for the Ser residues as well as Ala residues. The Ser residues in this silk fibroin are located at the position adjacent to PLA chain or close to the PLA chain,[2] and therefore Ser residues are incorporated into α-helix before structural transition of PLA chain. This is similar to the case of *A. pernyi* silk fibroin reported previously.[28] On the other hand, the conformation of the Tyr residues is expected to be random coil because Tyr residues are located at the center of Gly-rich sequence and mainly GYG sequence. Actually, the Cα chemical shift of Tyr residues, approximately 55 ppm, is close to the random coil chemical shift before and after structural changes.[33] Furthermore, it is noteworthy that Ala Cβ peak of *S. c. ricini* silk fibroin fiber is broad and asymmetric, which is similar to the Ala Cβ peak in the ^{13}C CP/MASR spectrum of *B. mori* silk fibroin fiber.[16,17] This reflects the heterogeneous structure of *S. c. ricini* silk fibroin fibers.

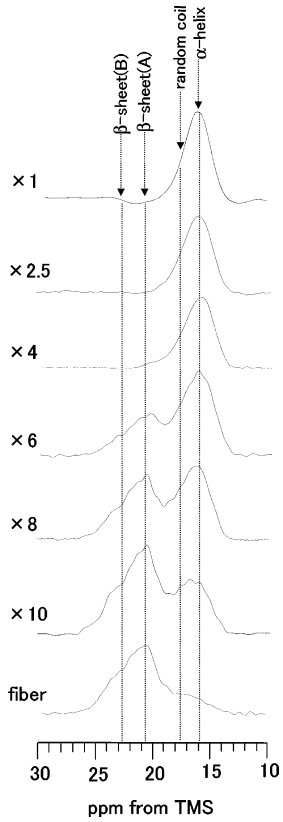

Figure 5. Expanded ^{13}C CP/MAS NMR spectra (Ala Cβ region) of *S. c. ricini* silk fibroin films with different stretching ratio (×1, ×2.5, ×4, ×6, ×8, and ×10) and *S. c. ricini* silk fibroin fiber.

The spectral change in the Ala Cβ peak was expanded and shown in Figure 5. With increasing the stretching ratio, the β-sheet structure appears clearly from the samples with the stretching ratio more than ×6. This is due to the appearance of the peaks at 20.8 ppm (β-sheet (A)) and 22.8 ppm (β-sheet (B)). Thus, all three different analytical data, that is, X-ray diffraction, Raman, and ^{13}C CP/MAS NMR data, show that the structure transition occurs remarkably for the silk fibroin samples with stretching ratio more than ×6. However, X-ray diffraction and Raman spectra are relatively sensitive to long-range order or periodic structure in the sample, but solid-state NMR is sensitive to the local structure. So the decrease in longer α-helix

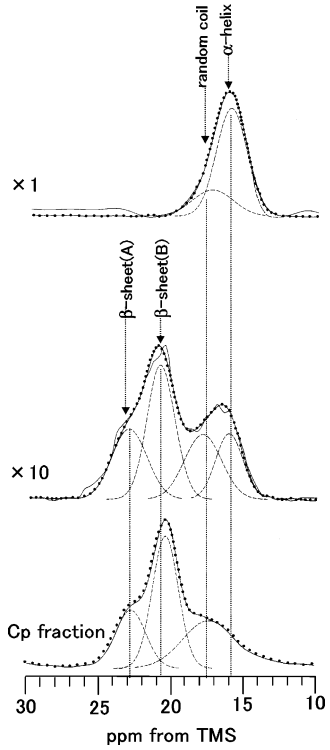

Figure 6. Spectral decomposition (broken lines) of Ala Cβ peaks of *S. c. ricini* silk fibroin without stretching (×1) and with stretching ratio (×10) together with that of the crystalline fraction (Cp fraction) of *B. mori* silk fibroin in silk II form.[16,17]

sequences in the sample reflects strongly in the X-ray diffraction and Raman spectra compared with the case of NMR. Figure 6 shows the decomposition of the Ala Cβ peak of the silk fibroin without stretching ×1 and with stretching ratio ×10 by assuming Gaussian line shape. The peak decomposition reported previously[16,17] for the crystalline fraction of *B. mori* silk fibroin with silk II form was also shown as a reference. The decomposition of the Ala Cβ peak of the silk fibroin without stretching ×1 indicates that the main structure is α-helix (15.7 ppm), but there are significant amounts of random coil (17.5 ppm), while the Ala Cβ peak of the sample with stretching ratio ×10 can be decomposed to four components: α-helix, random coil, and β-sheet (20.8 ppm (A) and 22.8 ppm (B)). The chemical shifts of the latter three peaks are basically the same of the corresponding three peaks observed in the crystalline fraction of *B. mori* silk fibroin with silk II form. The absence of the peak at 15.7 ppm in the ^{13}C CP/MAS NMR spectrum of *B. mori* silk fibroin is reasonable because of the absence of the α-helical region. It is interesting that the α-helical region still remains in the *S. c. ricini* silk fibroin with stretching ratio ×10.

Change in the Fraction of Four Peaks with Changing Stretching Ratio. The similar decomposition was performed for the Ala Cβ peaks of *S. c. ricini* silk fibroin with different stretching ratios including the silk fiber. The fraction of four components was plotted against stretching ratio as shown in Figure 7. The structural transition from α-helix to β-sheet occurs remarkably at the stretching ratio between ×4 and ×6 as mentioned above. The fractions of both peaks assigned to β-sheet increase gradually with keeping the ratio of relative intensities, approximately 2:1, with increasing stretching ratio in the cases of more than ×6. Reversely, the fraction of the α-helix peak decreases

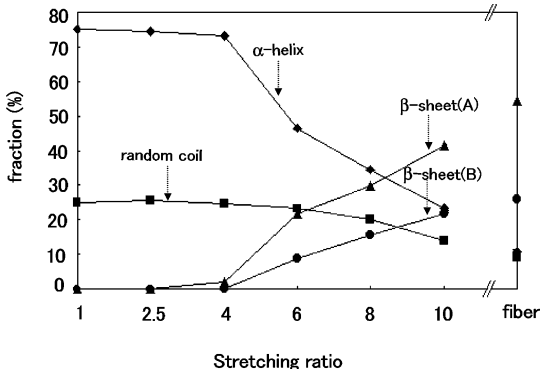

Figure 7. Changes in the fractions of four components in Ala Cβ peak with changing the stretching ratio: ◆, α-helix; ■, random coil; ▲, β-sheet (A, 20.8 ppm); ●, β-sheet (B, 22.8 ppm). The fraction for the silk fiber is also shown.

rapidly at the stretching ratio, more than ×6, and that of the random coil peak decreases gradually. The fraction of β-sheet in the fiber is considerably larger than that in the silk fibroin with stretching ratio ×10. After extrapolating each fraction against stretching ratio, it is expected that the fractions of the silk fiber correspond to the silk sample with stretching ratio ×12. Thus, α-helix and random coil conformations still remain even in the fiber. In our previous papers,[14,15] we reported that the Ala residues at the N- and C-terminus of PLA regions take a slightly different helix and contribute to the formation of $i \rightarrow i + 3$ hydrogen bonding. This special conformation seems to stabilize the α-helix formation of PLA region. This may be the reason why the α-helix still remains even in *S. c. ricini* silk fibroin fiber.

MD Simulation of Structural Change in the PLA Region of *S. c. ricini* Silk Fibroin Induced by Stretching. MD simulation is very effective to study the conformational change of silk fibroin by external forces as reported for *B. mori* silk fibroin previously.[18,19] So we will apply the MD simulation to the study on the structural transition of *S. c. ricini* silk fibroin. In our previous papers,[14,15] the 34-mer peptide with the sequence GGAGGGYGGDGG$(A)_{12}$GGAGDGYGAG was used as the model of the PLA region for structural determination with several solid-state NMR techniques such as 2D spin-diffusion NMR and REDOR. Thus, such a sequence can also be considered as a model peptide for MD simulation, but we used the more simple model peptide AGGAGG$(A)_{12}$GGAGAG.

The MD simulation of the structural transition of the model peptide was performed by changing the tensile strength. It should be noted that *S. c. ricini* silk fibroin samples were prepared by stretching in the presence of water molecules after the silk fibroin was took out from the silk gland. Then the ^{13}C CP/MAS, Raman, and X-ray diffraction data were obtained for the dried samples. Thus, we should take into account this experimental condition in the process of the MD simulation. Actually, the dried silk samples could not be stretched. Figure 8 shows Ramachandran maps of the conformational probability distributions of Ala residues in the model peptide in the presence of water molecules from 80 to 100 ps after MD calculation under different tensile stresses. The conformation of the Ala residues did not change under 0.1 GPa of tensile stress (Figure 8a) and α-helix conformation (the region of α_R; $(\varphi, \psi) = (-60°, -60°)$) was dominant. Under tensile stress 0.3 GPa, several conformations (C_5: $(\varphi, \psi) = (-150°, 150°)$, P_{II}: $(\varphi, \psi) =$

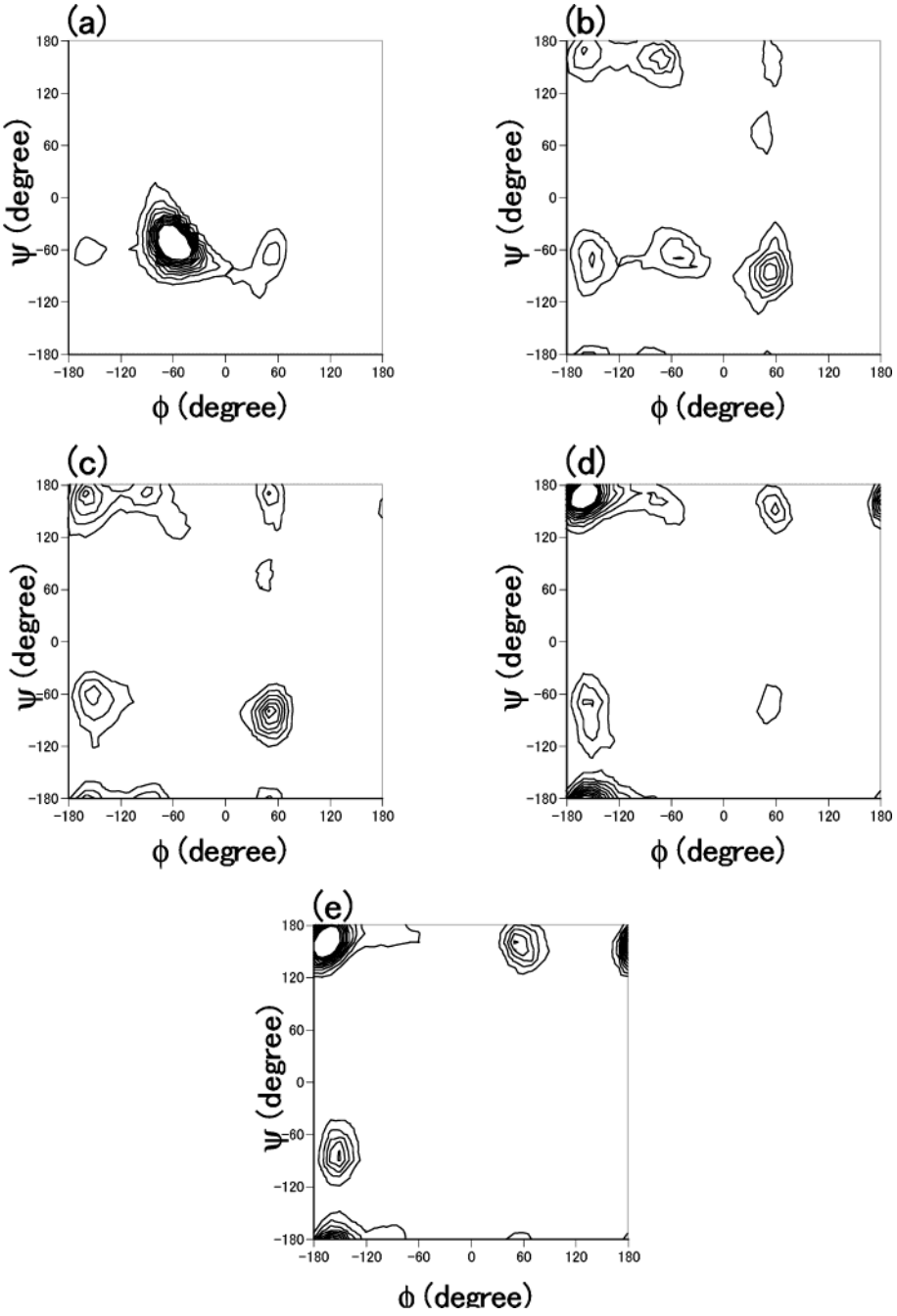

Figure 8. Conformational probability maps of Ala residues in model peptide, AGGAGG$(A)_{12}$GGAGAG, from 80 to 100 ps after MD simulation under different tensile stress (a) 0.1, (b) 0.3, (c) 0.5, (d) 0.8, and (e) 1.0 GPa in the presence of water molecules. Details of the MD calculation are described in the text.

(−60°, 130°), and α′ (φ, ψ) = (−150°, −60°) and $C7^{ax}$: (φ, ψ) = (60°, −70°)) were appeared except for α_R, and the most stable conformation was $C7^{ax}$ (Figure 8b). Then the α-helix conformation disappeared under tensile stress 0.5 GPa, and the fractions of $C7^{ax}$ and C_5 conformations increased (Figure 8c). As shown in Figures 8d,e, under more than 0.8 GPa of the tensile stress, the C_5 region ((φ,ψ) = (−150°, 150°)) were dominant together with significant amounts of the appearance of the conformation, α′ and another conformation with (φ, ψ) = (60°, 150°).

For each case, water molecules were removed, and then the MM calculation was performed again. Figure 9 shows change in Ramachandran maps of the conformational probability distributions of Ala residues in the model peptide after removal of water molecules. The typical character of the conformational distribution of Ala residue calculated with MD by changing tensile stresses in the presence of water still remains after the MM calculation in the absence of water molecules. However, there are significant differences between Figures 8 and 9 for each case of individual tensile stress. For example, another conformation with (φ, ψ) = (−60°, 60°) appeared in Figure 9b, and the conformation with (φ, ψ) = (60°, 150°) tends to disappear in Figure 9d,e. Figure 9a seems to reflect the conformational distributions of the silk fibroin samples without stretching or with stretching ratio ×2.5 in Figure 4, and the structure of *S. c. ricini* silk fibroin is predominantly α-helix. The decrease in the fraction of α-helix and appearance of

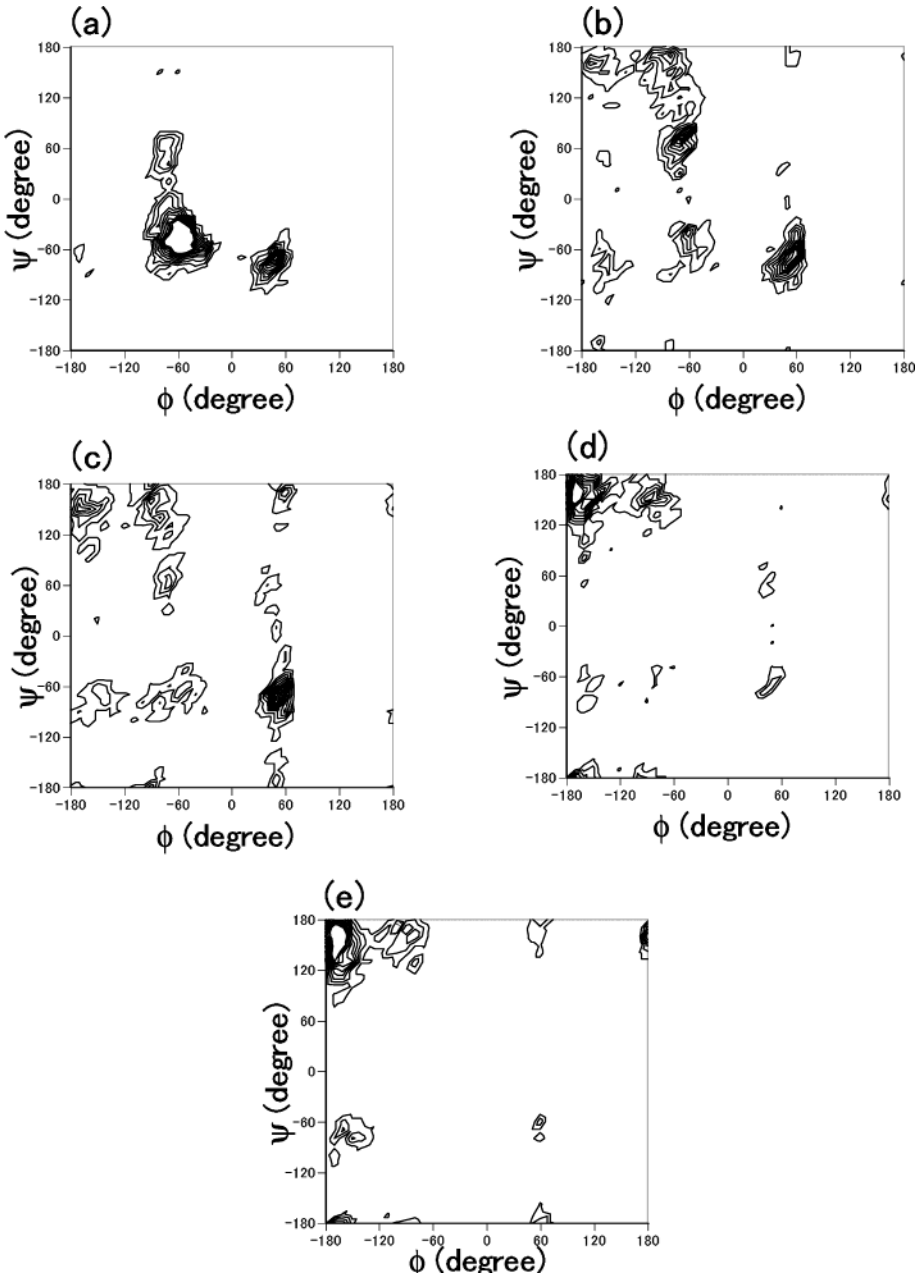

Figure 9. Conformational probability maps of Ala residues in model peptide, $AGGAGG(A)_{12}GGAGAG$, after MM calculation under different tensile stress (a) 0.1, (b) 0.3, (c) 0.5, (d) 0.8, and (e) 1.0 GPa after removal of water molecules. Details of the MD and MM calculations are described in the text.

β-sheet structure could be reproduced in Figure 9b, which corresponds to the conformational distribution of the samples $\times 6$ and $\times 8$. In the observed spectrum, a significant amount of α-helix conformation still remains in the sample $\times 10$ and silk fiber. Only Figure 9c predict the presence of α-helix conformation, and there are no α-helix region in Figure 9d,e. Thus, the MD calculation under more than the tensile strength 0.8 GPa cannot reproduce the conformational distribution of the silk fiber, and the calculation under 0.5 GPa seems to be valid for prediction of the conformation of the silk fiber. It is interesting to know the critical force for the structural transition of *S. c. ricini* silk fibroin experimentally. However, these experiments were reported only for *B. mori* silk fibroin. Magoshi et al.[20] have studied the relationship among stretching rate, stretching ratio, and critical force for the structural transition of *B. mori* silk fibroin prepared from the silk gland. The structural transition to β-sheet occurs at the stretching rate more than 1 cm/s, and the critical force was about 18 gf when the stretching rate was more than 1 cm/s. Thus, the critical force might be about 18 gf under our experimental condition 5−10 cm/s of the stretching rate although we used liquid silk taken from *S. c. ricini* instead of *B. mori* liquid silk. However, the fiber formation should be discussed by taking into account shear stress at the press part of spinneret and also the presence of metal ions other than the stretching force discussed here.

About two peaks at 20.8 and 22.8 ppm observed in β-sheet region of the Ala Cβ region, it is difficult to assign these peaks exactly. However, the difference in the intermolecular arrangement of Ala residues in the crystalline region of *S. c. ricini* silk fibroin might be the

possible reason as well as the case of *B. mori* silk fibroin with silk II structure. A further study is required to clarify this assignment.

Conclusion

The structural transition of *S. c. ricini* silk fibroin induced by stretching was monitored with ^{13}C CP/MAS NMR, X-ray diffraction, and Raman methods. Especially, the Ala Cβ region in the ^{13}C CP/MAS NMR spectrum gives a more quantitative discussion on the structural transition through the determination of α-helix, random coil, and two kinds of β-sheet structure in the polyalanine region. The change in the structure could be well-interpreted from the MD and MM calculations by taking into account the presence and absence of water molecules and application of tensile stress to the sample.

Acknowledgment. The authors acknowledge Dr. Yasumoto Nakazawa for stimulating discussions and Prof. Kenji Okuyama and Dr. Keiichi Noguchi for X-ray diffraction observation and supports from Insect Technology Project and Asahi Glass Foundation, Japan.

References and Notes

(1) Gosline, J. M.; Guerette, P. A.; Ortlepp, C. S.; Savage, K. N. *J. Exp. Biol.* **1999**, *202*, 3295−3303.
(2) Yukuhiro, K. Personal communication.
(3) Yukuhiro, K.; Kanda, T.; Tamura, T. *Insect Mol. Biol.* **1997**, *6*, 89−95.
(4) Sezutsu, H.; Yukuhiro, K. *J. Mol. Evol.* **2000**, *51*, 329−338.
(5) Asakura, T.; Murakami, T. *Macromolecules* **1985**, *18*, 2614−2619.
(6) Asakura, T.; Kashiba, H.; Yoshimizu, H. *Macromolecules* **1988**, *21*, 644−648.
(7) Asakura, T.; Yoshimizu, H.; Yoshizawa, F. *Macromolecules* **1988**, *21*, 2038−2041.
(8) Nakazawa, Y.; Asakura, T. *FEBS Lett.* **2002**, *529*, 188−192.
(9) Nakazawa, Y.; Nakai, T.; Kameda, T.; Asakura, T. *Chem. Phys. Lett.* **1999**, *311*, 362−366.
(10) Saito, H.; Iwanaga, Y.; Tabeta, R.; Narita, M.; Asakura, T. *Chem. Lett.* **1983**, 427−430.
(11) Ishida, M.; Asakura, T.; Yokoi, M.; Saito, H. *Macromolecules* **1990**, *23*, 88−94.
(12) Asakura, T.; Ito, T.; Okudaira, M.; Kameda, T. *Macromolecules* **1999**, *32*, 4940−4946.
(13) Van Beek, J. D.; Beaulieu, L.; Schafer, H.; Demura, M.; Asakura, T.; Meier, B. H. *Nature (London)* **2000**, *405*, 1077−1079.
(14) Nakazawa, Y.; Bamba, M.; Nishio, S.; Asakura, T. *Protein Sci.* **2003**, *12*, 666−671.
(15) Nakazawa, Y.; Asakura, T. *J. Am. Chem. Soc.* **2003**, *125*, 7230−7237.
(16) Asakura, T.; Yao, J. *Protein Sci.* **2002**, *11*, 2706−2713.
(17) Asakura, T.; Yao, J.; Yamane, T.; Umemura, K.; Ulrich, A. S. *J. Am. Chem. Soc.* **2002**, *124*, 8794−8795.
(18) Yamane, T.; Umemura, K.; Asakura, T. *Macromolecules* **2002**, *35*, 8831−8838.
(19) Yamane, T.; Umemura, K.; Nakazawa, Y.; Asakura, T. *Macromolecules* **2003**, *36*, 6766−6772.
(20) Magoshi, J.; Magoshi, Y.; Nakamura, S. *J. Appl. Polym. Sci.: Appl. Polym. Symp.* **1985**, *41*, 187−204.
(21) Parrinello, M.; Rahman, A. *J. Appl. Phys.* **1981**, *52*, 7182−7190.
(22) Swope, W. C.; Andersen, H. C.; Berens, P. H.; Wilson, K. R. *J. Chem. Phys.* **1982**, *76*, 637−649.
(23) Andersen, H. C. *J. Chem. Phys.* **1980**, *72*, 2384−2393.
(24) Yamane, T.; Inoue, Y.; Sakurai, M. *Chem. Phys. Lett.* **1998**, *291*, 137−142.
(25) Kondo, Y.; Hirabayashi, K.; Iizuka, E.; Go, Y. *Sen-I Gakkaishi* **1967**, *23*, 311−315.
(26) Hirabayashi, K.; Kondo, Y.; Go, Y. *Sen-I Gakkaishi* **1967**, *23*, 199−203.
(27) Hirabayashi, K.; Ishikawa, H.; Kasai, N.; Kakudo, M. *Kogyo Kagaku Zashi* **1970**, *73*, 1381.
(28) Nakazawa, Y.; Asakura, T. *Macromolecules* **2002**, *35*, 2393−2400.
(29) Monti, P.; Taddei, P.; Freddi, G.; Asakura, T.; Tsukada, M. *J. Raman Spectrosc.* **2001**, *32*, 103−107.
(30) Monti, P.; Freddi, G.; Bertoluzza, A.; Kasai, N.; Tsukada, M. *J. Raman Spectrosc.* **1998**, *29*, 297.
(31) Freddi, G.; Monti, P.; Nagura, M.; Gotoh, Y.; Tsukada, M. *J. Polym. Sci., Part B: Polym. Phys.* **1997**, *35*, 841−847.
(32) Tsukada, M.; Freddi, G.; Monti, P.; Bertoluzza, A. *J. Polym. Sci., Part B: Polym. Phys.* **1995**, *33*, 1995−2001.
(33) Asakura. T.; Sugino, R.; Yao, J.; Takashima, H.; Kishore, R. *Biochemistry* **2002**, *41*, 4415−4424.

MA049787U